
This is an electronic reprint of the original article.
This reprint may differ from the original in pagination and typographic detail.

Huan, Siqi; Zhu, Ya; Xu, Wenyang; McClements, David Julian; Bai, Long; Rojas, Orlando J.

Pickering Emulsions via Interfacial Nanoparticle Complexation of Oppositely Charged Nanopolysaccharides

Published in:
ACS Applied Materials and Interfaces

DOI:
[10.1021/acsami.0c22560](https://doi.org/10.1021/acsami.0c22560)

Published: 17/03/2021

Document Version
Peer-reviewed accepted author manuscript, also known as Final accepted manuscript or Post-print

Published under the following license:
Unspecified

Please cite the original version:
Huan, S., Zhu, Y., Xu, W., McClements, D. J., Bai, L., & Rojas, O. J. (2021). Pickering Emulsions via Interfacial Nanoparticle Complexation of Oppositely Charged Nanopolysaccharides. *ACS Applied Materials and Interfaces*, 13(10), 12581-12593. <https://doi.org/10.1021/acsami.0c22560>

This material is protected by copyright and other intellectual property rights, and duplication or sale of all or part of any of the repository collections is not permitted, except that material may be duplicated by you for your research use or educational purposes in electronic or print form. You must obtain permission for any other use. Electronic or print copies may not be offered, whether for sale or otherwise to anyone who is not an authorised user.

Pickering Emulsions *via* Interfacial Nanoparticle Complexation of Oppositely Charged Nanopolysaccharides

Siqi Huan,^{1,2,} Ya Zhu,³ Wenyang Xu,³ David Julian McClements,⁴ Long Bai,^{1,2,*} Orlando J. Rojas^{2,3,*}*

¹Key Laboratory of Bio-based Material Science and Technology of Ministry of Education, College of Material Science and Engineering, Northeast Forestry University, Harbin, Heilongjiang 150040, P. R. China

²Bioproducts Institute, Departments of Chemical & Biological Engineering, Chemistry, and Wood Science, 2360 East Mall, The University of British Columbia, Vancouver, BC V6T 1Z3, Canada

³Department of Bioproducts and Biosystems, School of Chemical Engineering, Aalto University, P.O. Box 16300, FIN-00076 Aalto, Espoo, Finland.

⁴Biopolymers and Colloids Laboratory, Department of Food Science, University of Massachusetts, Amherst, MA, 01003, USA

ABSTRACT

We consider the variables relevant to adsorption of renewable nanoparticles and stabilization of multiphase systems, including particle's hydrophilicity, electrostatic charge, axial aspect, and entanglement. Exploiting the complexation of two oppositely charged nanopolysaccharides, cellulose nanofibrils (CNF) and nanochitin (NCh), we prepared CNF/NCh aqueous suspensions and identified the conditions for charge balance (turbidity and electrophoretic mobility titration). By adjusting the composition of CNF/NCh complexes close to net neutrality, we produced sunflower oil-in-water Pickering emulsions with adjustable

droplet diameter and stability against creaming and oiling-off. The adsorption of CNF/NCh complexes at the oil/water interface occurred with simultaneous partitioning (accumulation) of CNF on the surface of the droplets in net negative or positive systems (below and above stoichiometric charge balance relative to NCh). We further show that the morphology of the droplets and size distribution were preserved during storage for at least 6-months at ambient conditions. This long-term stability was held with a remarkable tolerance to changes in pH (e.g., 3 ~ 11) and ionic strength (e.g., 100 ~ 500 mM). The mechanism explaining these observations relates to the adsorption of CNF in the complexes, counteracting the charge losses resulting from the deprotonation of NCh or charge screening. Overall, CNF/NCh complexes and the respective interfacial nanoparticle exchange greatly extend the conditions favoring highly stable, green Pickering emulsions that offer potential in applications relevant to foodstuff, pharmaceutical, and cosmetic formulations .

KEYWORDS: nanochitin, cellulose nanofibrils, Pickering emulsions, interfacial adsorption, pH tolerance, salt resistance, food emulsions

INTRODUCTION

Emulsions belong to thermodynamically nonequilibrium systems,¹ that might display long-term kinetic stability.² In practice, molecular-based emulsifiers are utilized to reduce the interfacial tension between immiscible phases,³ preventing or delaying their separation.⁴ Pioneering work by Ramsden⁵ and Pickering⁶ demonstrated emulsion stabilization using particles with dimensions in the colloidal size range, referred to as Pickering emulsions. Particles exhibiting similar wettability for water and oil phases (balanced contact angles) show

a strong tendency to achieve irreversible adsorption at interfaces.⁷ This produces an interfacial steric barrier, preventing droplet coalescence or breakage,⁸ which allows high colloidal stability.⁹ Upon preparation, Pickering emulsions often undergo limited coalescence.⁹⁻¹¹ This occurs when oil/water interfaces are formed, displaying a much larger area compared to what can be potentially covered by the particles. As the formation of the droplets is halted, those that are (partially) unprotected start to coalesce, gradually reducing the total interface between water and oil phases. Moreover, stabilization of Pickering droplets is also able to be achieved *via* forming robust networks within the continuous phase involving particle bridging and entanglement,^{12,13} which can prevent or delay droplet movement. These unique attributes of Pickering stabilization are beneficial for green multiphase systems because Pickering emulsion can achieve sufficient stability without requiring molecular stabilizers that are often synthetic.¹⁴ Hence, Pickering emulsion offer a versatile platform for developing and optimizing multiphase products, for instance, foodstuff, pharmaceutical, and cosmetic multiphase systems.

The colloidal particles used so far for Pickering stabilization include those made from modified natural or synthetic polymers,^{15,16} as well as inorganic particles.¹⁷ However, the growing preference for label-friendly ingredients, particularly in foodstuff,¹⁸ has increased the demand for new choices,¹⁹ expanding the interest in other particle stabilizers, especially if derived from natural and renewable resources.¹⁴ Among the latter, plant-based particles are promising candidates,^{20,21} owing to their abundance, sustainability, biodegradability, and nontoxicity.²² For instance, cellulose nanocrystals (CNC) have been shown to form and stabilize different types of Pickering systems.^{23,24} Likewise, more flexible and longer cellulose

nanofibrils (CNF) have also been considered,²⁵⁻²⁷ particularly if used in their unmodified forms.²⁸⁻³¹

Compared with CNC, CNF is noted to have a reduced efficiency as Pickering stabilizer.³² Some of the reasons for this observation include the larger dimensions (axial aspect) of CNF, together with its inherent tendency for entanglement,³³ and strong hydrophilicity,³⁴ all of which prevent CNF diffusion and adsorption at oil/water interfaces.³⁵ For the same reasons, CNF is usually applied as a rheological modifier.³⁶ Nevertheless, when used as an emulsifier, CNF stabilizes oil droplets with a loose coverage, leading to droplets with sizes in the micron range,²⁸ which tend to cream and coalesce. Furthermore, it is possible for non-adsorbed or free cellulose nanofibrils dispersed in the continuous, aqueous phase to induce flocculation of oil droplets *via* depletion forces,³⁷ thereby impairing emulsion droplet morphology and flow behavior. It thus follows that CNF adoption in Pickering stabilization can be further facilitated *via* increasing CNF affinity with the oil/water interface, for example, by hydrophobization or surface modifications.³⁸ Unfortunately, such treatments reduce the sustainability prospects, especially considering food, cosmetic and green emulsions. In sum, it remains significantly challenging to endow CNF with the interfacial affinity required in stable, green Pickering emulsions.

Physical adsorption, for instance, by electrostatic interaction, facilitates nanoparticle adsorption at interfaces.³⁹ It has been demonstrated that food-grade Pickering emulsions can be stabilized by CNC electrostatically-modified with cationic surfactants;⁴⁰ however, to the best of our knowledge, no attempts have been attempted for CNF. Beyond this concept, rather

than surfactants, and especially considering label-friendly products, particles or biopolymers bearing cationic charges can be combined with CNF. An option is the naturally-derived chitin, a cationic, insoluble polysaccharide bearing surface acetyl amine group groups.^{41,42} Among colloidal nanoparticles derived from chitin,⁴³ fibril-like nanochitin (NCh) can be easily produced by mechanical disintegration under acidic condition. Moreover, the effectiveness of NCh in stabilizing the oil/water interfaces has been demonstrated given its interfacial wettability,⁴⁴ leading to high droplet surface coverage.^{45,46} While NCh is a good Pickering stabilizer on its own,⁴⁷⁻⁵⁰ there is the possibility to tailor its interfacial adsorption if it is combined with other components, such as CNF.⁵¹⁻⁵³ In fact, here we propose such systems to achieve enhanced stability, for example, to variations in pH and ionic strength.

Herein, we enhance interfacial adsorption by *in situ* electrostatic complexation of CNF with cationic NCh. We hypothesize that the interfacial adsorption of such CNF/NCh complexes can be controllably tuned by using the mass/charge ratio of CNF to NCh, going from a dominant dispersed system in the aqueous phase to a strongly associated system, both providing stable Pickering multiphase systems. To our knowledge, this report is the first attempt to combining two naturally-derived nanopolysaccharides to facilitate their interfacial adsorption and tailorable Pickering stabilization. While NCh is sensitive to pH and salinity, for instance, the colloidal stability of NCh originates from the electrostatic repulsion, which can be reduced by deprotonation at high pH (loss of surface charge) and by charge screening at high salinity,⁵⁴ the complexation of NCh with CNF is expected to create all-renewable stabilization of green Pickering emulsions with great environmental tolerance. In this study,

we offer an in-depth understanding of the interactions between NCh with CNF, as oppositely-charged nanopolysaccharides, aiming at the design, optimization, and manufacture of all-renewable Pickering emulsions.

EXPERIMENTAL SECTION

Materials. Raw, unpurified blue crabs were obtained from a supermarket in Helsinki, Finland. Meanwhile, wood pulp (bleached sulfite birch fibers) was supplied as a source to produce cellulose nanofibrils (CNF), following a previous report.⁵⁵ The fibers were bleached, free of fines and supplied in a never-dried form. The fibers were subjected to microfluidization (M110P, Microfluidics Int. Co., MA) using six passes (1500 bar). Note: no fiber pretreatment, either chemical or enzymatic, was applied prior to microfluidization. The obtained CNF suspension was kept at 4 °C until use. The averaged lateral diameter of the CNF was appr. 28 ± 4 nm, with lengths being from submicrons (several hundreds of nanometers) to several microns (**Figure S1a**). Other chemicals, including HCl, acetic acid (100%), NaOH, NaCl, Calcofluor white stain solution, Nile red powder, styrene (St), and azobis(isobutyronitrile) (AIBN) were acquired from Sigma Aldrich (Helsinki, Finland). For the oil phase, the choice of sunflower oil considered our previous work and facilitated comparisons.^{23,45} The sunflower oil was obtained from a supermarket. All of the chemicals considered in our experiments were used without additional purification. The water ($18.2 \text{ M}\Omega \cdot \text{cm}$) used to prepare the emulsions was obtained by filtration using a Millipore unit and herein referred to as water, unless indicated otherwise.

Nanochitin preparation. α -chitin from fresh crabs was purified according to a previous report.⁴² In brief, unpurified shells from fresh crabs were immersed in 24-h cycles in 1 M HCl and 1 M NaOH solutions to remove minerals (e.g., calcium) and proteins. At least three cycles were used. The processed shells were further decolorized using NaClO₂ solution (0.5 wt%, pH 5.0 with acetic acid) for at least 2 h at 70 °C. After decolorization, residues of purified chitin shells were thoroughly cleaned using running distilled water (hot and cold) to remove impurities. Finally, the obtain chitin, in forms of flakes, were crushed into small pieces using a kitchen blender.

In this study, the chitin nanoparticles that were obtained by mechanical disintegration are referred to as nanochitin (NCh). The procedure applied to produce NCh was slightly modified according to our recent report.⁵⁶ In brief, small pieces of purified chitin were deacetylated with NaOH solution (33 wt%) at 90 °C. The total reaction time was set to 3.5 h based on our previous experience. The solid-to-liquid ratio was fixed at 0.04 g/mL. After deacetylation, partially-deacetylated chitin was obtained, herein referred to as DE-chitin, which was fully cleaned by running hot and cold water until reaching pH of 7 or lower. Then an overnight dialysis was performed to further remove impurities from the obtained DE-chitin. The acetylation degree of DE-chitin was approximately 72.5%, similar to the value determined by conductivity titration in our earlier efforts.⁴⁵ Before mechanical nanofibrillation, DE-chitin was dispersed in acidic water (0.2 wt% concentration) to achieve full protonation of the surface amine groups, which resulted in a “coarse” DE-chitin suspension. The pH (3.0) of the suspension was adjusted using acetic acid under continuous stirring. After re-dispersion, the coarse suspension of DE-chitin

was further homogenized at room temperature with the aim of generating finer fibrils. This was carried out with a homogenizer (T-25, Digital Homogenizer, IKA, Germany). The obtained fine DE-chitin suspension was further disintegrated into NCh *via* ultrasonication with a high-power tip sonicator (Sonifier 450, Branson Ultrasonics Co., USA) using a 50% power strength relative to the maximum power. The sonication duration in this experiment was set to 40 min alternately using 5 s on and 2 s off. The obtained NCh suspension was kept in 4 °C fridge prior to analysis and use. The dimensional data of obtained NCh were 170 ± 30 nm in length and 12 ± 2 nm in width (**Figure S1b**).

CNF/NCh complexes. CNF stock suspension (1.7 wt%) was diluted to 0.5 wt% using water. NCh suspensions were prepared by diluting NCh stock suspension (0.6 wt%) to given concentrations with water at pH 3.0 (acetic acid). The suspensions composed of CNF/NCh complexes and produced under given conditions are listed in **Table 1**. Therein, the CNF/NCh complexes are named as “CN-x”, with x representing the respective conditions (10 different systems). The complexation of CNF with NCh was produced by mixing 0.5 wt% CNF suspension with that of NCh at the given concentration and using a volumetric ratio of 1:1 for a total of 10 ml. Subsequently, CNF/NCh suspension was vortexed and then sonicated for 5 min at 25 °C using a bath sonicator (DT 52/H, Sonorex Digitec, Germany). For all obtained complex suspensions, the final pH was fixed at pH=3.0 by addition of acetic acid. A reference sample, 0.25 wt% CNF suspension, was obtained by dilution with water of the 0.5 wt% CNF suspension. The CNF/NCh complex suspensions were kept at room temperature until further analysis and use (digital photos for suspensions were taken after storing for at least 12 h).

Table 1. Composition and zeta potential of CNF/NCh complexes in suspensions prepared at the given condition¹

Code	C_{F-NCh} (wt%)	$C_{F-CNF/NCh}$ (wt%)	Mass ratio	$\zeta_{Suspension}$ (mV)	$\zeta_{Emulsion}$ (mV)
CN-1	0	0.25	-	-62 ± 2	-56 ± 1
CN-2	0.0005	0.2505	500/1	-61 ± 1	-51 ± 1
CN-3	0.0025	0.2525	100/1	-25 ± 1	-32 ± 1
CN-4	0.005	0.255	50/1	-21 ± 0.3	-24 ± 1
CN-5	0.025	0.275	10/1	58 ± 1	29 ± 1
CN-6	0.05	0.3	5/1	82 ± 2	44 ± 0.7
CN-7	0.1	0.35	2.5/1	89 ± 2	49 ± 0.5
CN-8	0.15	0.4	5/3	91 ± 0.6	50 ± 1
CN-9	0.2	0.45	5/4	91 ± 1.5	52 ± 1
CN-10	0.25	0.5	1/1	0.25	0.5

¹ C_{F-NCh} are the concentrations of NCh in the final suspension. $C_{F-CNF/NCh}$ stands for the total concentration of nanopolysaccharides in the final suspension. For all suspensions, the final concentration of CNF is 0.25 wt%.

Complex colloidal stability. *ζ -potential.* The ζ -potential of CNF/NCh complexes formed in the respective suspensions was assessed by dynamic light scattering (ZS-90, Malvern Instruments, UK). In order to avoid multiple scattering effects, the samples were diluted using water before measurement. The averaged results were obtained by using freshly prepared samples (duplicate samples) with three runs for each sample.

Turbidity. The turbidity of the CNF/NCh complex suspensions was measured with a UV-vis spectrophotometer (UV-2550, SHIMADZU, Japan) operated at room temperature. The transmittance for all of the samples was measured at 600 nm. The samples were placed in an optical cell with 1-cm path length. The turbidity was calculated based on previous reports according to the below equation.⁴⁰

$$\text{Turbidity} = 2.3 \times \log \frac{1}{T}$$

where T stands for the transmittance of the sample. The results were averaged by measuring three freshly prepared samples that were prepared within 2h before testing.

Morphology. The microstructure of CNF, NCh and CNF/NCh complexes was observed using normal transmission electron microscope (TEM, JEM-2800, JEOL, Japan) with a 120 kV acceleration voltage. Briefly, the respective suspension was diluted to 0.005% using water, and then a drop of the sample was deposited on the TEM grid that was coated with carbon-based formavar film. The sample was further negatively stained using an uranyl acetate solution before drying the grid at room temperature.

CNF/NCh-stabilized Pickering emulsions. Pickering emulsions were produced with the respective CNF/NCh complexes, used as stabilizer (see **Table 1**) and the sunflower oil (10 to 50 wt%) as the oil phase. Briefly, certain amount of oil phase was loaded into a plastic tube that was filled with the respective CNF/NCh suspension, and then emulsification of the two phases was by microtip sonication (Sonifier 450, Branson Ultrasonics Co., USA). The microtip was placed close to the top surface of the fluid. The input power was fixed at 40% strength of the maximum power of the sonicator (determined by heat balance, that is, the increase of temperature with reaction time) by alternating 5 s on and 2 s off, for total 60 s. In order to minimize overheating during ultrasonication, the plastic tube was placed in an ice-water throughout the emulsion preparation. A reference sample that was stabilized by 0.25 wt% NCh was also prepared following the same procedure. The visual appearance of the emulsions was accessed within 24 h after sample preparation. The long-term stability of the emulsions following long-term storage at room conditions was determined following any phase separation

and recorded with photos of the emulsions after at least 6-months, a standard time used to evaluate the stability of foodstuff emulsions.⁵⁷

Optical fluorescent microscopy was used to identify the oil phase and CNF/NCh complexes. For this purpose, the sunflower oil was dyed with Nile red solution (1 mg/mL in ethanol). Prior to emulsification, the Nile red solution was directly loaded into sunflower oil at a ratio of 1/50, and the mixture was vigorously stirred at room temperature for at least 12h.

For accessing the surface morphology and identifying the nanopolysaccharides adsorbed at the surface of the droplets, we prepared CNF/NCh-stabilized Pickering emulsions using styrene (St) as the dispersed phase. The oil phase was then polymerized (radical polymerization), forming polystyrene (PS) beads. Briefly, the aqueous phase was the same as that used in the respective sunflower oil emulsions (composed of the CNF/NCh complexes). Meanwhile the oil phase contained St and the initiator (AIBN) (AIBN-to-St ratio of 1/100 w/w). For emulsion preparation, 1 g of St/AIBN mixture was mixed with 9 g of the CNF/NCh complex suspension. The two phases were emulsified using the same procedure used for the sunflower oil emulsions. In order to minimize the influence of air trapped in the system, the obtained St-in-water emulsions were degassed for at least 10 min using nitrogen gas before the start of the polymerization at 65 °C. The polymerization of St into PS was let to occur for 24 h at 65 °C in the absence of stirring.

Pickering emulsion stability. In order to evaluate Pickering emulsion stability against environmental stresses, fresh CNF/NCh-stabilized emulsions containing sunflower oil (10 wt%) were subjected to different conditions of pH and salinity (ionic strength). The CNF/NCh

complex suspension used (CN-10 sample) corresponded to a total concentration of CNF/NCh of 0.5 wt%. The respective emulsion (at least 20 mL) was loaded into a container, following pH adjustment using HCl or NaOH solutions (pH 3 to 11). The salinity or ionic strength (0 to 500 mM) was adjusted by NaCl addition. After vortexing, the emulsions were transferred into transparent glass vials for visual observation. Before analysis, the emulsions were held for 24 h holding time at room temperature.

Emulsions characterization. *Droplet sizing.* The mean droplet diameter of the emulsions and corresponding size distribution were measured by static light scattering (Mastersizer 2000, Malvern Instruments, UK). In order to avoid multiple scattering effects, the respective emulsions were diluted with water for analysis. The refractive indices of the aqueous phases and the sunflower oil used were assumed to be 1.33 and 1.47, respectively. The mean droplet size was calculated as the Sauter mean diameter ($D_{32} = \sum n_i d_i^3 / \sum n_i d_i^2$) using the full size distribution range. Particularly, the span of the samples was reported based on the width of particle size distribution. To facilitate the comparison among samples, corresponding droplet size distributions were shifted vertically using sizing data from the same initial droplet volume. The measurements were conducted in triplicate using freshly prepared samples.

Microscopy. The morphology of the emulsions after storage and at different environmental stresses was observed from images obtained by confocal laser scanning microscopy (Leica DMRXE, Leica, Germany) using an oil immersion objective lens (60×). The sample (100 µL) that was obtained from the top layer of the emulsion was dyed using Nile red solution (10 µL) before observation. The dyed sample was equilibrated for at least 10 min at room temperature

after gentle mixing using a pipette. Then, 6 μL of the stained sample was deposited on a clean microscope slide and a glass coverslip was used to cover the sample, under no load. After the sample was evenly spread, the coverslip was immediately fixed using transparent nail polish. This procedure was applied to minimize evaporation of water or solvent. The excitation/emission spectra for Nile red used in this study were 488/539 nm.

The sunflower oil droplets and CNF/NCh complexes in the samples were simultaneously imaged with a fluorescent optical microscope (Zeiss Axio Observer, Zeiss, Germany) with an oil immersion objective lens ($63\times$). Prior to emulsion preparation, the sunflower oil was dyed with Nile red solution, leading to red-stained samples. Before observation, nanopolysaccharides were dyed with Calcofluor white solution. The procedure used for preparing dual-stained samples was the same as that used for confocal imaging. The excitation/emission spectra for Calcofluor white used in this study was 365/435 nm, respectively. The fluorescence signals in the images (red and blue) were processed by ImageJ code (imagej.nih.gov), which was used to generate merged images.⁵⁸ In some images, the red color was too strong, and became dominant over the other, resulting in a blurred merged image of the blue contour. Note: owing to the large sample volume deposited onto the glass slide needed for observation, overlapping of multiple droplets is unavoidable. This represents a challenge for interpretation (confounding with flocculation). To account for this effect, the morphology of the droplets was additionally accessed by using CLSM.

To analyze the surface of the polymerized PS beads, scanning electron microscopy (SEM, Zeiss Sigma VP, German) was used with an accelerated voltage of 1 to 2 kV. Briefly, a drop

of the diluted emulsion (100-fold) was deposited onto the sample holder, following overnight drying at ambient temperature. Before SEM observation, the dried PS beads were sputter-coated with platinum/palladium.

RESULTS AND DISCUSSION

CNF/NCh complexation. The addition of NCh to a CNF suspension under conditions away from net neutrality produced colloiddally stable systems (**Figures 1a** and **1b**), with no visible phase separation, flocculation or sedimentation. The measured turbidity of the suspensions (1.6) only increased slightly compared to that of the initial CNF suspension (**Figure 1b**). Thus, the colloidal stability of CNF (0.25 wt% suspension) was not significantly affected upon complexation with NCh, provided the charge of the system was net negative or positive. These results are mainly attributed to relatively strong inter-particle electrostatic repulsion in aqueous media, given the high surface charge of the respective complexes, as shown **Figure 1b**. ζ -potential of the CN-1 system was ca. -60 mV, slightly lower than that of the neat CNF suspension (-62 mV) (**Table 1**) and high enough to ensure strong electrostatic stabilization. As expected, the increased NCh addition (CN-3 and CN-4), produced complexes with less negative ζ potential (-25 mV). Further addition of NCh, for example, in sample CN-5, produced a shift in the sign of the net charge (the ζ potential shifted to positive), indicating that the transition point for charge compensation or balance occurs at a condition between those on CN-4 and CN-5 samples. We deliberately avoided such condition leading to complex charge neutrality, occurring in a very small window of NCh concentration (NCh suspensions at a concentration between 0.01 and 0.05 %, **Table 1**). Under these narrow conditions, phase

separation occurs, making the suspension less effective for the purpose of Pickering emulsion stabilization. Overall, the results indicate excellent colloidal stability of CNF/NCh complexes below or above net zero charge. The latter condition takes place in a narrow concentration range and implies that NCh can be conveniently added to tailor the net charge of the complexes following protocols such as those used in colloidal titration.

The typical morphology of CNF/NCh complexes for CN-8, which are net positive, is shown in the TEM image (**Figure 1c**). Comparing such morphology with that of neat CNF or NCh (**Figure S1**), it is apparent that no significant aggregation occurred, which is in line with the turbidity measured in the aqueous suspension. It should be noted that while no visible flocs were observed in suspensions just below and above charge neutrality (NCh concentrations of 0.01 to 0.05 wt%, **Table 1**), small visible aggregates could be identified after diluting the suspensions. This was the result of such complexes being subjected to weak electrostatic repulsion, favoring interparticle bridging and leading to CNF/NCh aggregates with dimensions in the micrometer scale. The latter significantly impaired identification of the complex microstructure. A similar aggregation phenomenon has been discussed in our previous report.⁴⁰ In sum, colloidally stable CNF/NCh complexes were easily formed below and above the conditions for net zero charge (from -62 to +75 mV) by nanoparticle titration and are discussed next for Pickering stabilization.

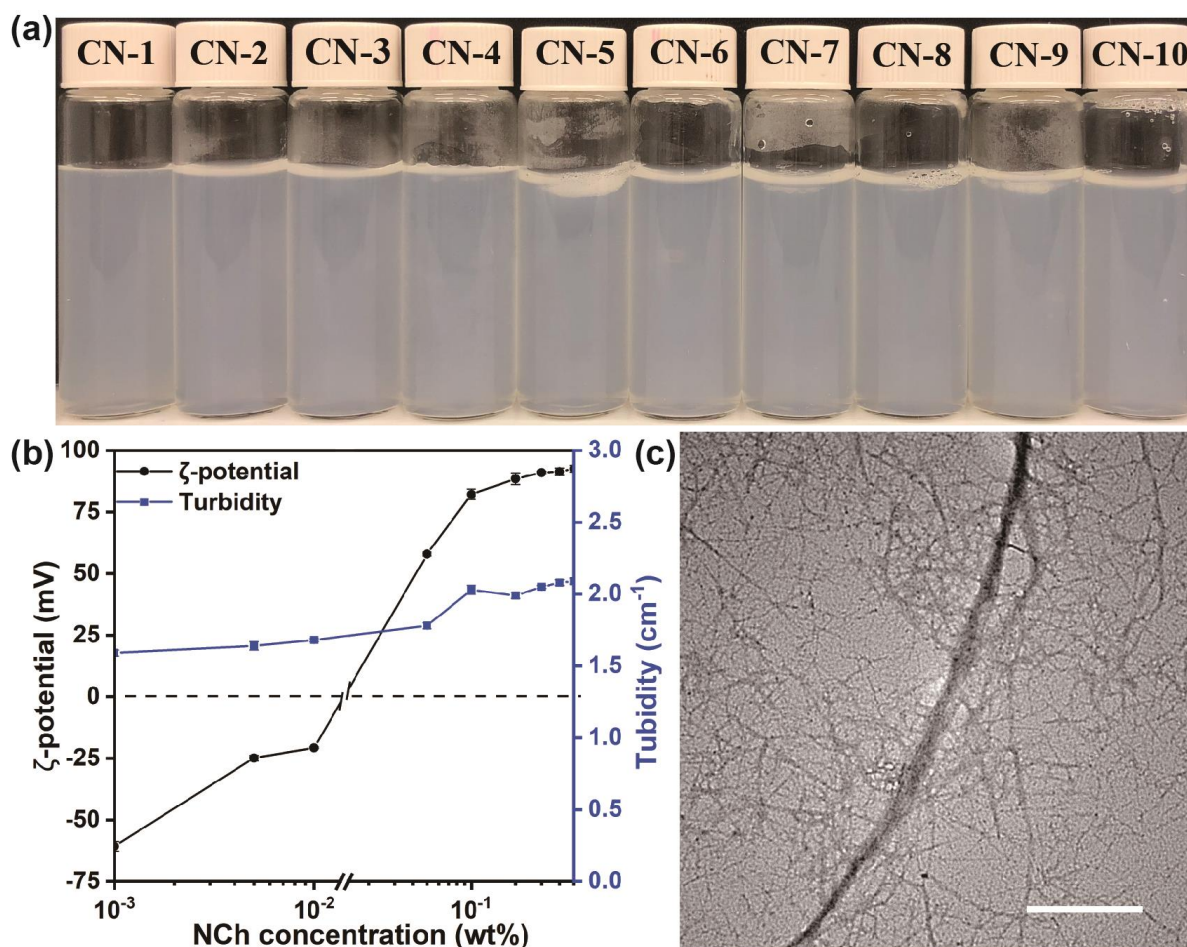


Figure 1. (a) Photograph and (b) plots of turbidity and ζ -potential (mV) of CNF aqueous suspensions at given NCh addition levels (**Table 1**). The respective CNF/NCh complex suspension is shown on each sample at increased loading of NCh (CN-1 to CN-10, from left to right). (c) Transmission electron microscopy of sample CN-8. The scale bar corresponds to 500 nm.

Pickering emulsions stabilized with CNF/NCh complexes. *Formation and stabilization.*

Sunflower oil-in-water Pickering emulsions were emulsified using sunflower oil (10 wt%) and the respective CNF/NCh complex suspension. **Table 1** refers to the initial CNF (0.5 wt%) and NCh (varying) concentrations. As shown in **Figure 2a**, the emulsion prepared with neat CNF was less stable than those produced with the complexes. Soon after preparation, oil coalescence and oiling-off occurred on top of the emulsion (see circled area in **Figure 2a**). By contrast, aqueous suspensions containing the CNF/NCh complexes resulted in stable emulsions (no

oiling-off nor creaming), even at very small addition level of NCh (CN-2 aqueous system with mass CNF/NCh ratio of 500/1, for example), indicating the excellent emulsifying ability of the complexes. Furthermore, the emulsions stabilized with neat NCh (0.25 wt%) displayed a homogeneous appearance (**Figure S2**), pointing to the high stabilization capability of NCh in Pickering emulsions.^{45, 52}

Figure 2b includes mean droplet diameter (D_{32}) of the respective emulsions, which can be controlled *via* NCh titration. Here we use the net ζ -potential of the CNF/NCh complexes as a parameter to compare the properties of the emulsions. When the emulsions were stabilized with CNF/NCh complexes with decreased net negative ζ -potential (CN-2 to CN-5), the droplet size became larger compared to that of pure CNF. Particularly, the emulsions stabilized with CN-4 and CN-5 showed considerably larger droplet size. Two main factors are likely responsible for this observation. Firstly, relatively large CNF/NCh complexes that formed at near neutral conditions limited their transport from the continuous, aqueous phase to the newly formed oil/water interfaces and afterwards their adsorption.^{25,59} As a result, the oil droplets initially formed during sonication would significantly coalesce soon after sonication, resulting in large droplets. It should be noted that while complexes with lower surface charges may promote the adsorption at the oil/water interfaces, a balance between limited transport and reduced interparticle electrostatic repulsion should be considered. Secondly, droplet coalescence during formation and storage occurred as a consequence of weak electrostatic repulsion between the droplets, given a reduced surface charge of droplets that were stabilized by less charged CN-4 and CN-5 (**Table 1**). Under conditions of zero net charge, the droplets are expected to be

extremely large. While such samples were not prepared, the anticipated initial droplet size can be indicated to belong somewhere in the area indicated by the dotted line in **Figure 2b**. Using the CNF/NCh complexes with high net charge (CN-6 and beyond), the droplet size was significantly reduced. The complex with the highest (positive) charge tested (CN-10) produced emulsions with very small droplet size (3 μm), much smaller than those produced from neat CNF. The results indicate the benefit of NCh in emulsifying complexes. Regardless of the droplet size, all the Pickering emulsions prepared were homogeneous and stable with no signs of phase separation (**Figure 2a**). This is partially attributed to the high viscosity and viscoelasticity of the emulsions (**Figure S3**), which prevented coalescence and restricted oiling-off during storage.

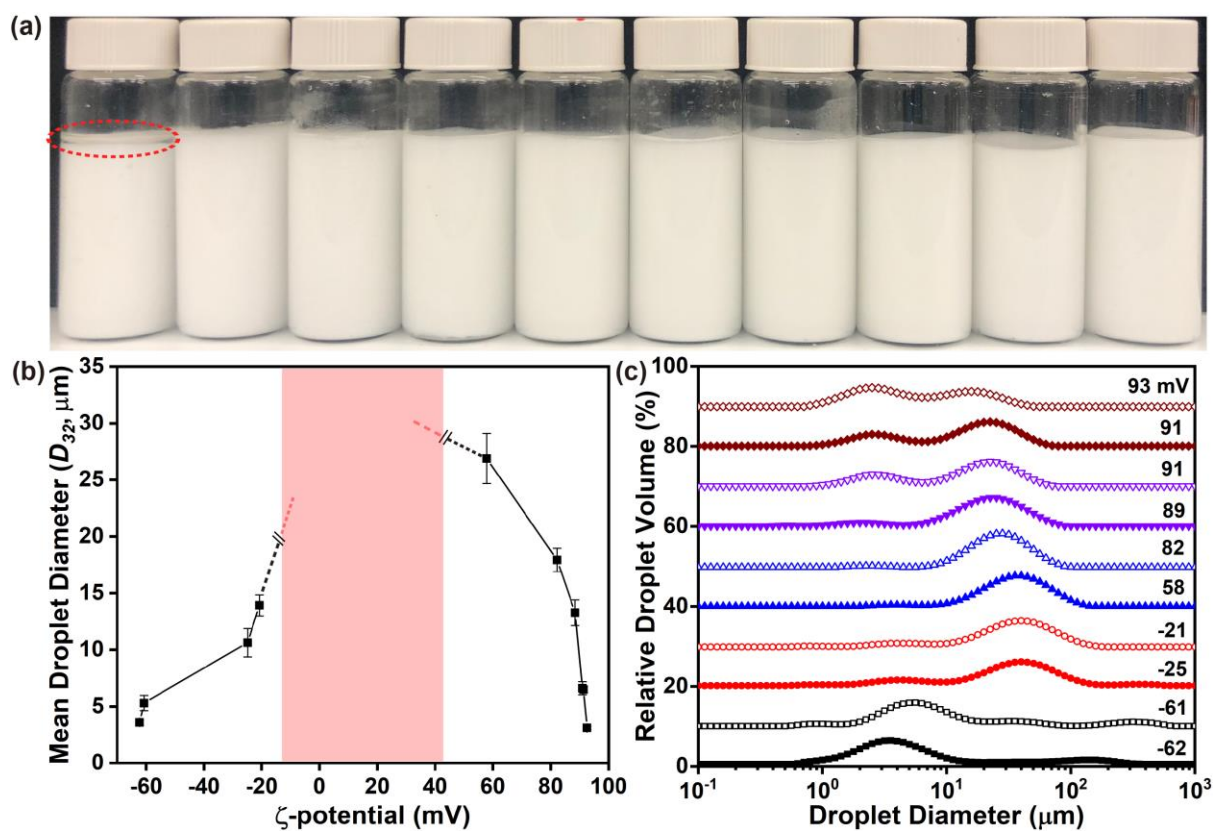


Figure 2. (a) Photograph and (b) plots of mean droplet diameter (D_{32}), and (c) corresponding size distributions of CNF/NCh-stabilized sunflower oil-in-water Pickering emulsions (10 wt% oil phase)

with given CNF/NCh ratios in the aqueous phase (CN-1 to CN-10, from left to right). The red dashed circle in (a) shows oiling-off. The net ζ -potential values (mV) of the CNF/NCh complexes were used in the x axis of the mean droplet size (b) and as labels in the respective distributions (c). The dashed lines in the colored area in (b) is added as a guide to indicate a possible evolution in initial diameter of droplets of emulsion prepared with CNF/NCh complexes under close to neutral net charge (ζ -potential = 0).

Figure 2c illustrates the size distribution of emulsion droplets that were stabilized using the CNF/NCh complexes. The corresponding size distribution of droplets prepared at relatively large negative charge (CN-1 and CN-2) were multimodal (less uniform). By contrast, the droplet size distribution was monomodal in emulsions prepared with complexes loaded with NCh (less negatively charged or positively charged, samples CN-3 to CN-10). Noticeably, emulsions prepared with complexes with a net charge between -25 and +58 mV showed a wider size distribution (span of ~ 3), which indicate a higher polydispersity and lower stability. When using highly charged complexes (>89 mV), the droplet size showed a distribution with two apparent peaks, indicating the influence of two different mechanism for the formation of emulsion droplets with highly charged complexes. This result will be considered in the following section (**Figure 3** and **4**).

We next evaluate the morphology of CNF/NCh-stabilized Pickering emulsions by confocal imaging (**Figure S4**). The droplet size exhibited a similar trend as previous findings (**Figure 2b**). Emulsions stabilized with CNF/NCh complexes at a relatively large ζ -potential (CN-2 and CN-3) presented droplets that were well-dispersed and, compared to those produced with neat CNF, showed increased droplet diameter, which agreed with the data shown in

Figure 2b. Not surprisingly, for emulsions with low surface charge originated from the less charged complexes (CN-4 and CN-5) (**Table 1**), large clusters of oil droplets with polydisperse distribution and slightly irregular shapes were clearly identified. The emulsions prepared with complexes of high net ζ -potential, particularly CN-8 to CN-10 (> 90 mV), showed a reversed evolution of oil droplet diameter, that is, the droplet size became smaller and more uniform. This result therefore demonstrated the efficiency of such complexes in stabilizing Pickering emulsions. Overall, incorporation of NCh in complexed systems improves the emulsifying capability of CNF and achieve stable Pickering emulsions with adjustable droplet properties.

Stabilization mechanism of emulsion. We identified CNF/NCh complexes in the emulsions using a dual-channel fluorescent microscope after tagging the nanoparticles (blue) and the sunflower oil (red) (**Figure 3** and **Figure S5**). Once again, the results indicated excellent emulsion stability. According to the images shown in the blue channel and the merged images (see the blue, thin contour surrounding the oil droplets), and despite the multiple effect of dye reflection from aqueous phase, the CNF/NCh complexes were found to be distributed at the oil/water interfaces, for all NCh concentrations and regardless the droplet size. These results confirm the role of the CNF/NCh complexes in stabilizing Pickering emulsion *via* interfacial adsorption. On the other hand, free CNF or respective complexes were present in the continuous, aqueous phase, particularly as identified from the blue channel images in **Figure 3** and **Figure S5**, which implied the formation of viscous, nanofibril networks in the aqueous phase, contributing to droplet stabilization (**Figure S3**).

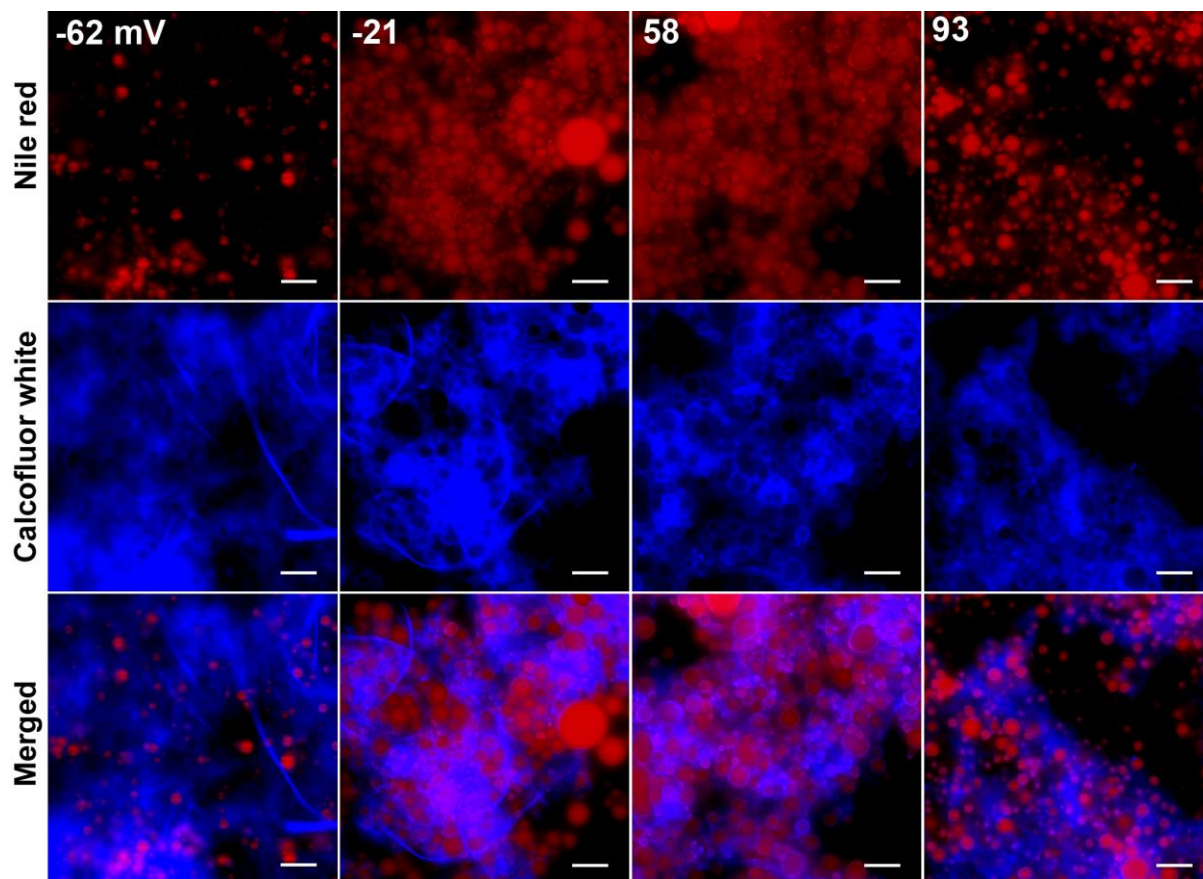


Figure 3. Fluorescent images of CNF/NCh-stabilized sunflower oil-in-water Pickering emulsions (10 wt% oil phase) with CNF/NCh complexes CN-1, CN-4, CN-5, and CN-10. The ζ -potential (mV) of CNF/NCh complexes is indicated in each image. The upper row corresponds to images from samples comprising stained oil, and the middle row corresponds to those with stained CNF/NCh complexes. The bottom row is a merged image obtained from the other two. The oil phase and the CNF/NCh complexes were stained following standard procedure using Nile red and Calcofluor white, respectively. Prior to observation, all samples were kept at ambient temperature for 24 h. The scale bar corresponds to 20 μ m.

We appraised the surface coverage of the CNF/NCh complexes following additional experiments using CNF/NCh-stabilized St-in-water Pickering emulsions, after polymerization of St to form spherical PS beads. This allowed for the fibrils to be identified on the surface (**Figure 4** and **Figure S6**). Moreover, the trends in bead size agreed with our findings of complex-stabilized sunflower oil-in-water systems (**Figure 3** and **Figure S4**). It should be

noted that the small beads observed in the images relate to the polymerization of St monomer that was extruded through the surface of the droplets.⁶⁰ Such monomer was polymerized in the aqueous phase wherein thermally activated AIBN initiated the reaction and the free, isolated CNF/NCh complexes functioned as nucleation sites.

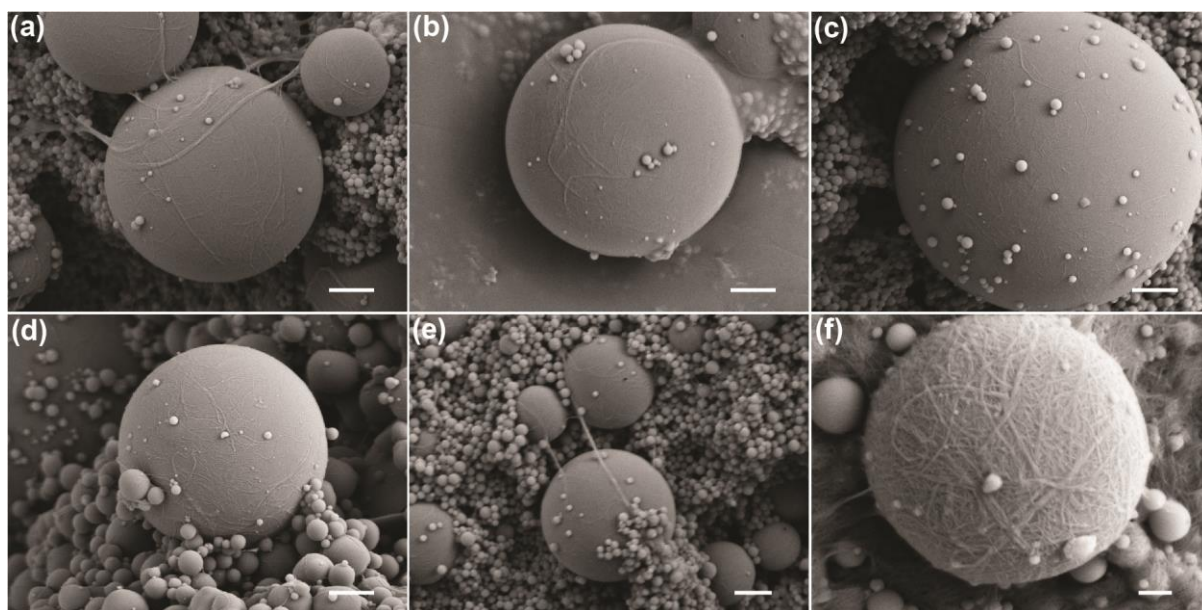


Figure 4. Scanning electron microscope (SEM) images of polymerized St-in-water Pickering emulsions that were stabilized by CNF/NCh complexes at (a) CN-1, (b) CN-4, (c) CN-5, and (d) CN-10. (e) PS beads showing inter-connected CNF (CN-4 case). (f) SEM image of smaller droplets in emulsions stabilized with CN-10, indicating a bimodal droplet size distribution. The scale bar in (a) to (e) corresponds to 1 μm , and in (f) is 200 nm.

An interesting observation in the fluorescence images was the contribution of blue reflection in the continuous, aqueous phase of Pickering emulsions stabilized at low NCh concentrations (or pure CNF). They indicate the presence of free nanofibrils (**Figure 3** and **Figure S5**). A question that arises is how NCh enables tunable interfacial adsorption of CNF/NCh complexes, from randomly dispersed fibrils in the continuous, aqueous phase to tightly adsorbed complexes at the sunflower oil/water interfaces. A mechanism that might

explain such effect is illustrated schematically in **Figure 5**. Free CNF dispersed in the continuous, aqueous phase, shown as long and flexible nanofibrils, given a relatively large (negative) ζ -potential (**Figure 1b** and **Figure S1b**). When neat CNF was used for emulsion preparation, some oil droplets appeared interconnected by the free, dispersed CNF (**Figure 3**), as supported by SEM images of PS beads stabilized by pure CNF (**Figures 4a, 4e** and **Figure S6a**), which shows a loose networked organization at the surface as well as inter-particle connections. By loading NCh, the complexation, *via* electrostatic interaction between NCh and CNF, gradually leads to a partial coverage of CNF by NCh, as indicated by the change in ζ -potential (**Figure 1b**). Meanwhile, the acetyl groups on the surface of NCh retained in the complexes, acting as hydrophobic sites with better affinity to the oil phase,⁴⁵ presumably improving complex adsorption at the interfaces, with their hydrophilic entities interacting with the water phase (**Figure 5b**). When surface charge of the CNF/NCh complexes was still negative, at low NCh addition (CN-2 to CN-4) (**Figure 1b** and **Table 1**), more CNF surfaces were exposed, favoring for CNF to remain partially dispersed in the continuous, aqueous phase (left illustration in **Figure 5a**). Thus, such system was less efficient for interfacial adsorption of CNF. Moreover, the hydrophilic nature and large dimension of CNF/NCh complexes limit their diffusion from the continuous, aqueous phase to the oil/water interfaces and afterwards their adsorption.

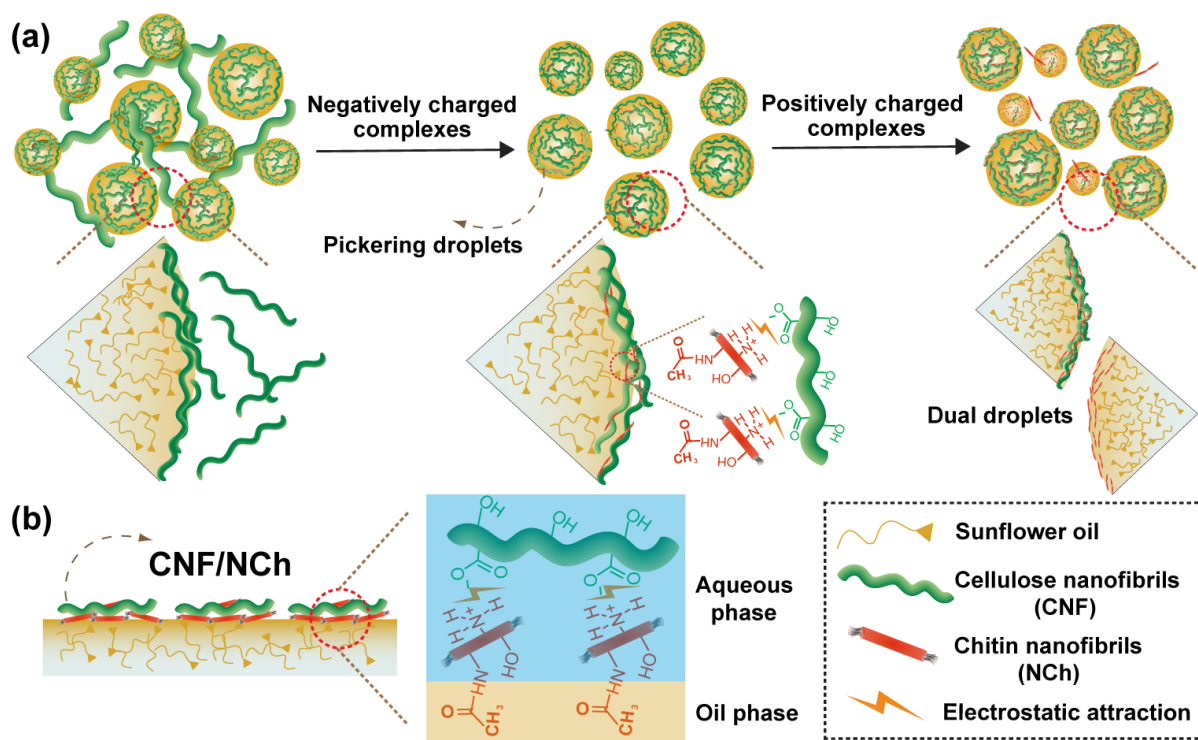


Figure 5. (a) Depiction of the possible mechanisms involved in the formation and stabilization of oil droplets in a continuous, aqueous phase, e.g., Pickering emulsions stabilized with CNF/NCh complexes of given charges (the illustrations are not to scale). The charge balance of the complexes affects their interfacial adsorption. (b) Illustration of the interfacial adsorption of the CNF/NCh complexes. Affinity between acetyl groups (hydrophobic entities) in NCh and the oil phase is expected to facilitate complex adsorption and interfacial coverage of CNF at the interface.

The CNF surface was considered to be fully covered by NCh when the ζ -potential of CNF/NCh complexes shifted to positive (**Table 1** and **Figure 1b**). In such case, no complexes, particularly fibril-like CNF bundles, were identified in the continuous, aqueous phase (**Figure 3** and **Figure S5**). Therefore, based on the NCh's nature,⁴⁵ it is reasonable to assume that a more complete interfacial adsorption of the complexes can be achieved by means of the hydrophobic acetyl groups of NCh, close to the surface of the droplets (**Figure 5a**, center). However, even if NCh neutralizes CNF and improves emulsion stability, under conditions of low net surface charge near the transition point, the electrostatic repulsion is weaker and leads

to an increased droplet size (**Figure 2b** and **Figure S4**). Indeed, a higher ζ -potential of positively-charged complexes leads to a reduction of emulsion droplet size and narrower droplet size distributions (**Figure 2b** and **c**). For complexes with ζ -potential > 90 mV, free NCh existed in the continuous, aqueous phase (excess NCh upon complexation). Confirmation is found from the reference system based on PS, where fully covered, smaller beads were observed for CN-10 system (**Figure 4f**). The bead size was similar to that of previous experiments conducted with neat chitin nanofibers,⁴⁵ thereby demonstrating the role of free NCh on droplet stabilization (**Figure 5a**, right panel). This result also explains the bimodal droplet size distribution observed at high NCh loadings (**Figure 2c**). In sum, this is the first report to demonstrate that complexation of NCh with CNF can controllably tailor the interfacial adsorption of the CNF/NCh complexes and produces stable Pickering emulsions. Hence, the complexation between oppositely-charged nanopolysaccharides is introduced here as an all-natural, efficient and novel system for green Pickering emulsions.

High oil fraction Pickering emulsions. We examined the performances of Pickering emulsions that were stabilized by the CNF/NCh complexes with varying water-to-oil ratio (WOR). The emulsions that were stabilized with the CNF/NCh complex (CN-10) at different oil fractions (WOR up to 50/50) showed high stability against creaming and oiling-off after storing at room temperature for 24 h (**Figure S7a**). Phase separation occurred in emulsions with WOR = 40/60. The droplet diameter and its distribution, as observed from **Figure S7b**, indicate that the diameter of the oil droplets gradually increased with the loading of oil, attaining 8.7 μm when WOR = 50/50 was used. This result is also confirmed by confocal

imaging (**Figure S8**). By increasing the oil phase fraction, the relative coverage of nanoparticles is reduced at given CNF/NCh complexes, which increases the likelihood of droplet coalescence during ultrasonication, finally resulting in larger droplets. Interestingly, the droplet size distribution shifted from bimodal at low oil fractions to unimodal at high oil loading. This is because at relatively low oil loading, the complexes and free NCh stabilized, separately, the oil droplets. In contrast, at high NCh levels, all the nanoparticles in the system were required to stabilize the newly generated interfaces, resulting in a relative even distribution of the complexes and free NCh. **Figure S7c** addresses the rheology of the emulsions of varying oil content and shows $G' > G''$ for all emulsions, which reveal the presence of emulsion gels. A synergistic effect is responsible for this result, from the contribution of (1) relatively high NCh loading in the complex and free NCh in the aqueous phase⁴⁵ and, (2) reduced free volume of the aqueous phase and enhanced inter-droplet interactions when the volume of the oil droplets was increased. This also explains the high stability of the emulsions against creaming and oiling-off during storage. To conclude, the CNF/NCh complexes are superior stabilizers of Pickering emulsions, even for systems with high oil fractions.

Environmental stress on the stability of Pickering emulsions. In practice, emulsions usually undergo a series of conditions during production, processing, storage, transportation, and use.^{2, 18} It is therefore pertinent to develop robust systems that resist alteration under changing conditions. In this context, one of the limitations of NCh-stabilized emulsions is limited pH stability, owing to the deprotonation and decreased surface charge at high pH.

Moreover, salt-induced charge screening of droplets covered by NCh impairs emulsion stability. So far, it is evident that 1) CNF is much larger than chitin nanoparticles used in this study (**Figure S1**); 2) CNF/NCh complexes efficiently adsorb at the oil droplets in Pickering emulsions, and 3) NCh drives interfacial adsorption of the complexes, given the affinity of the hydrophobic sites distributed on the NCh surface (**Figure 5b**). We hypothesize that complexation of CNF with NCh improves the tolerance of emulsions to shifts of pH and ionic strength (**Figure 6a**). As such, the behavior of emulsions under varying environmental stresses is discussed in the following sections.

Tolerance to pH. **Figure 6b** displays the effect of pH on the stability of CNF/NCh-stabilized Pickering emulsions. When adjusting the pH value to pH = 9, the emulsions prepared with pure NCh separated into serum (bottom) and creamed (upper) layers. In contrast, the CNF/NCh-stabilized emulsions were found to be stable against creaming and oiling-off visibly in the pH range from 3 to 11 (**Figure 6b**, insert), and the droplet size was only slightly increased to ~10 μm at pH 11 (**Figure 6b**). Moreover, confocal images confirmed that oil droplets that were stabilized by CNF/NCh complexes kept their shape and displayed high stability against droplet flocculation and oil coalescence, at least within the studied pH range (3-7) (**Figure 7**). At pH > 9, a slight flocculation occurred, as judged from the optical images (**Figure S9a**). These observations are in contrast to the behavior of emulsion droplets stabilized with pure NCh, which significantly flocculated at pH 9 (**Figure 7** and **Figure S9b**). Bearing in mind that changes in droplet size occurred at different pH, the results confirm the hypothesis that

CNF/NCh complexes enable positively-charged Pickering emulsions with extensive tolerance to changes in pH.

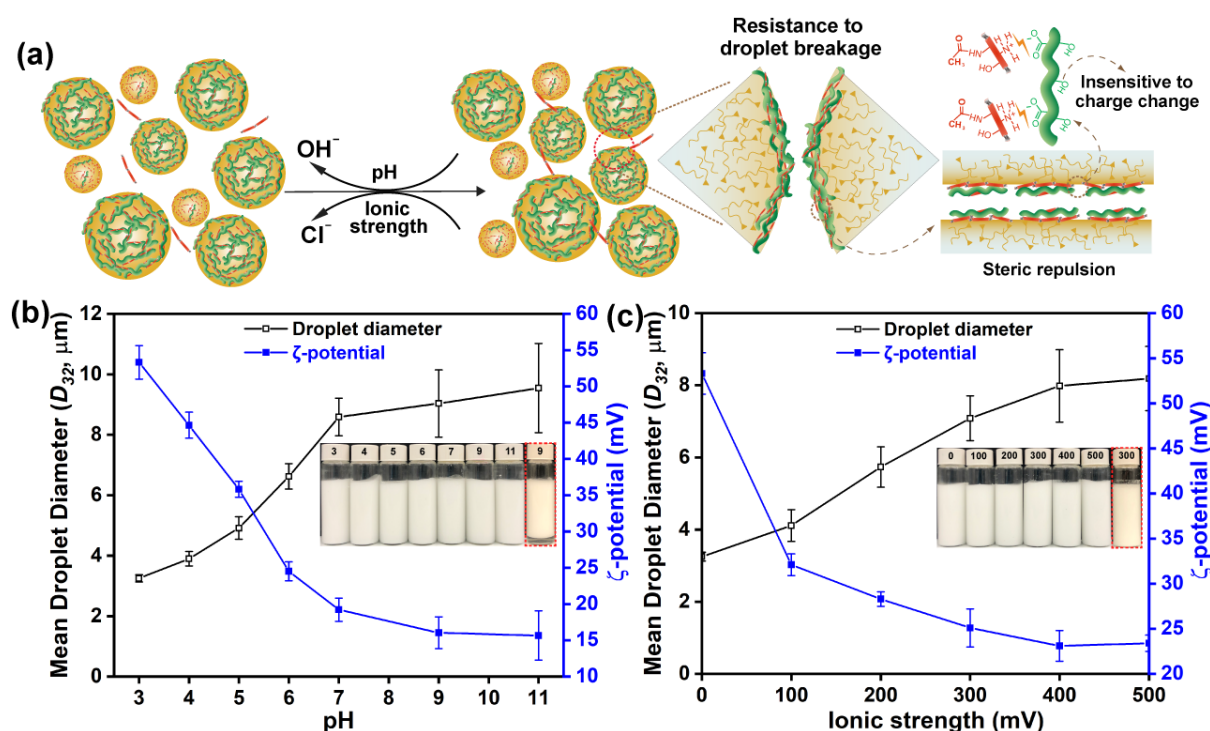


Figure 6. (a) Schematics showing (not to scale) the stabilization mechanism leading to the tolerance of CNF/NCh complex-stabilized emulsion droplets under varying environmental stresses. Such effect is the result of electrostatic repulsion and/or steric hindrance. Taken case of the emulsions stabilized by CNF/NCh complexes (CN-10) using sunflower oil (10 wt%), the figure in (b) shows mean particle diameter (D_{32}) and ζ -potential of emulsions at varying pH (3-11). Likewise, (c) corresponds to the influence of ionic strength (0-500 mM NaCl). Prior to characterization, all the samples were kept still at room temperature for 24 h. The inserted digital images in (b) and (c) were photographed after 24 h and include the emulsions at the given conditions (see labels). As reference, the visual appearance of emulsions that phase-separated or creamed are included, corresponding to systems stabilized with 0.25 wt% NCh at pH 11 and 500 mM NaCl, respectively (see red dashed square).

A question remains as to the reasons why CNF/NCh-stabilized emulsions tolerate changes in pH. As shown in **Figure 6b**, strong electrostatic repulsion at $\text{pH} \leq 6$ explains the stability of the droplets. As the pH increases, $\text{pH} > 7$, the relatively weak electrostatic repulsion partially

prevented droplet coalescence (even if the ζ -potential of the complexes decreased to approximately +15 mV). This is significantly different compared to the situation of pure NCh (ζ -potential < +5 mV). By its anionic nature, the presence of CNF in the complexes counterbalanced the deprotonation of NCh at high pH values, particularly over pH = 7. Moreover, the hydrophobic sites (acetyl groups) of NCh in the complexes enhance the interfacial adsorption. It can be speculated that the hydrophilic CNF in the complexes are structured close to the aqueous phase (**Figure 5b**), and considering the large aspect ratio of CNF, a strong short-range steric repulsion is generated, restricting coalescence (**Figure 6a**). We note that high storage modulus of CNF/NCh-stabilized emulsions is another factor limiting oil coalescence at high pH.

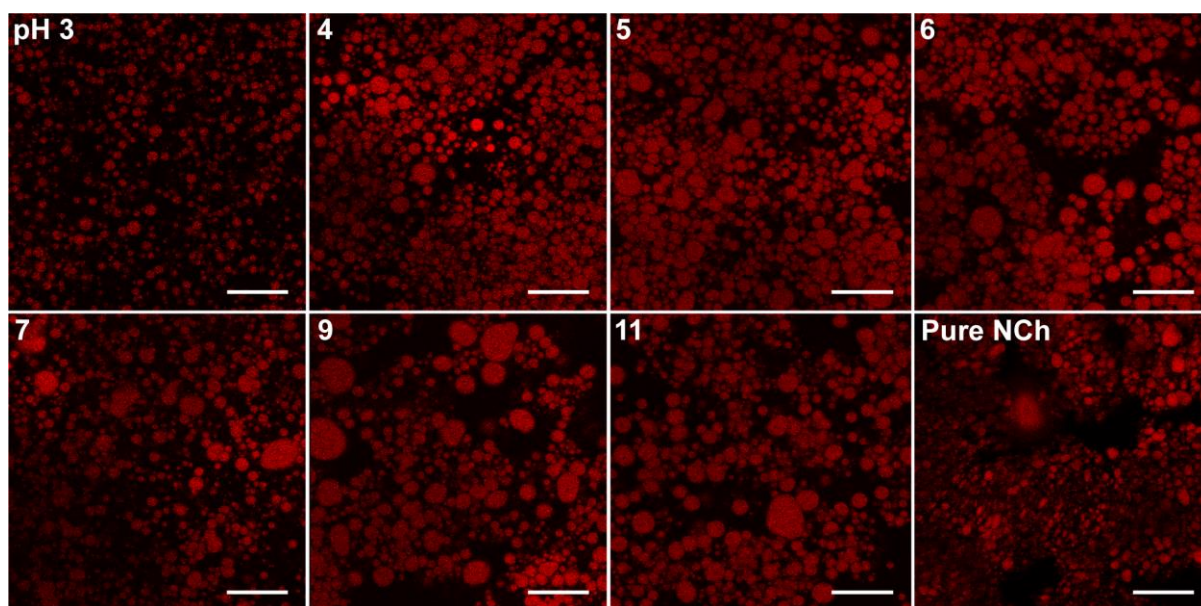


Figure 7. CLSM images of CNF/NCh-stabilized Pickering emulsions with varied pH (3 to 11). The emulsions were stabilized by CNF/NCh complexes (CN-10) and the sunflower oil (10 wt%). The image of an unstable emulsion is included as a reference (0.25 wt% “Pure NCh” at pH 9). Prior to characterization, all samples were kept at ambient temperature for 24 h. The scale bar corresponds to 20 μm .

Tolerance to salinity. The effect of the salinity on the stability of emulsions prepared with CNF/NCh complexes was investigated at different values of the ionic strength *via* varying NaCl concentration in the aqueous phase (**Figure 6c**). Visible creaming and oiling-off for neat NCh-stabilized emulsions were evident at 300 mM NaCl ionic strength (**Figure 6**, inset). Flocculation and coalescence of emulsion droplets occurred at a ζ -potential close to zero, under conditions of electrostatic screening. The significant flocculation, together with apparent oil coalescence, were confirmed by confocal imaging (**Figure S10**). In contrast, all CNF/NCh-stabilized emulsions were stable against creaming and oiling-off, regardless of the ionic strength; in fact, the mean particle diameter remained relatively small, even at 500 mM NaCl, as seen in **Figure 6c** (also confirmed by confocal micrographs, **Figure S10**). This result supports our hypothesis that CNF/NCh complexes enable Pickering emulsions with high resistance to ionic strength.

It should be noted that according to confocal imaging, a weak flocculation was seen at high ionic strength, e.g., 400 and 500 mM (**Figure S10**). It is likely that the large aggregation of droplets was not detected in the size measurement when using static light scattering, given that the dilution used for sample preparation. The strong tendency for the flocculation of the CNF/NCh-stabilized droplets at increased salinity is ascribed to electrostatic screening. In this condition, counterions tend to cluster around the cationic surfaces of droplets, as confirmed by the sharp decrease of ζ -potential (from ca. +55 to ca. +25 mV) with NaCl loading (**Figure 6c**). However, it should be noted that compared with the sample prepared with pure NCh, the charge screening of CNF/NCh complexes at elevated ionic strengths may be mitigated by the presence

of CNF.³² This can be attributed to the flexibility of large nanofibrils that adjust the configuration of the complexes at given salt loading, partially protecting the surface of the complexes from counterion clustering. Thus, this effect results in the occurrence of a weak electrostatic repulsion that resist complete droplet flocculation. This is significantly different compared with the case of the pure NCh sample. Similar as the effect of pH, the strong steric repulsion generated by CNF/NCh complexes adsorbed on the droplet surfaces and the viscoelasticity of CNF/NCh-stabilized emulsions restricted oil coalescence (**Figure 6a**), facilitating salt tolerance. In sum, the CNF/NCh complexes are shown as effective emulsifiers of Pickering emulsions, which exhibit high stability against the changes of pH and ionic strength, most useful in formulating all-green emulsion products.

Long-term stability of emulsions. Long-term stability of emulsions is a key factor when evaluating products, particularly for cosmetic, pharma and food applications. An expected shelf life of emulsion-based commercial food products, under typical storage conditions and at 30 °C, is usually taken to be at least 6 months.⁵⁷ Consequently, this criteria was used to evaluate the long-term storage stability of the sunflower oil-in-water Pickering emulsions that were stabilized by the CNF/NCh complexes. As shown in **Figure 8**, the stability of emulsions at varied NCh concentrations was demonstrated after 6-month storage. Emulsions stabilized with CNF alone showed oil coalescence, soon after preparation. The emulsions stabilized by the complexes were stable (visual observation) after 6-month storage (**Figure 8a**). The confocal images in **Figure 8b** show that most of the emulsions kept their droplet shape and were distributed homogeneously after 6 months, similarly as those of freshly prepared samples

(Figure S4). The samples prepared with the less charged CNF/NCh complexes (CN-2, CN-3 and CN-4) showed slight oil coalescence, resulting in the formation of irregular droplets. This was likely the result of decreased inter-droplet electrostatic repulsion. The high stability of CNF/NCh-stabilized Pickering emulsions is ascribed to their high storage modulus (Figure S3), similar to the case of emulsion gels (emulgels);⁴⁵ therein, the movement of droplets is locked during storage, restricting or at least delaying the creaming or coalescence.

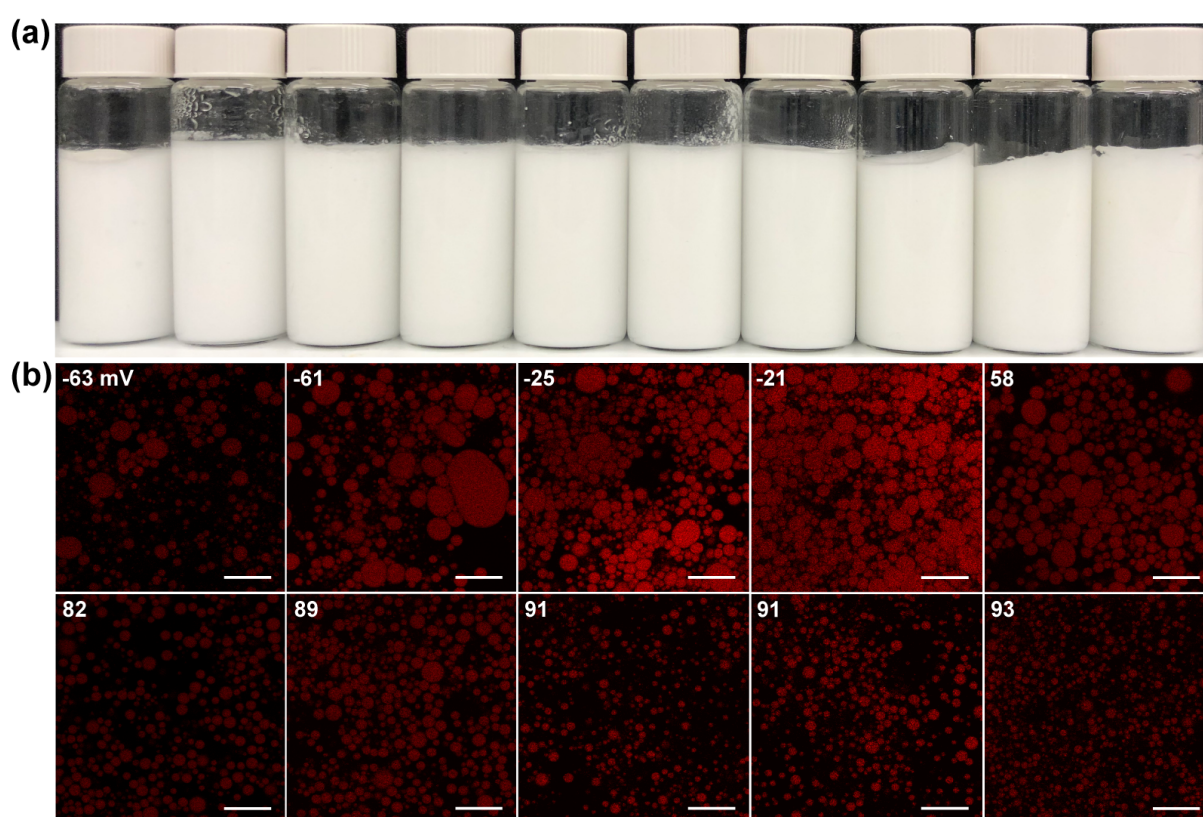


Figure 8. (a) Digital photos and (b) CLSM images of sunflower oil-in-water Pickering emulsions that were stabilized by the CNF/NCh complexes after 6-month storage. The emulsions were stabilized with CNF/NCh complexes (CN-1 to CN-10, from left to right in (a)). The ζ -potential (mV) of CNF/NCh complexes is indicated in each image in (b). All the emulsions were kept still at room temperature before characterization. The scale bar corresponds to 20 μm .

As shown in **Figure S11a**, emulsions of different internal oil fractions produced with CN-10 exhibited high stability against droplet creaming and separation of oil phase over 6 months. As seen from **Figure S11b**, compared to the corresponding fresh emulsions, the emulsions after storage still kept well-dispersed oil droplets (**Figures S8**). The diameter of the droplets also remained almost constant within the observation time, which is a result of the formation of emulsion gels at increased concentrations of the internal phase. The long-term storage stability of the CNF/NCh-stabilized Pickering emulsions, over at least 6 months, demonstrate the excellent prospects of CNF/NCh complexes as green, renewable stabilizer of Pickering multiphase materials.

CONCLUSIONS

Sunflower oil-in-water Pickering emulsions of high colloidal stability were prepared using different fractions of the internal phase and by combining oppositely-charged nanopolysaccharides (CNF and NCh). The CNF/NCh complexes showed colloidal stability in water, forming semi-transparent suspensions at given NCh concentrations, with a transition point for charge compensation between 0.01 to 0.05 wt% NCh. Pickering emulsions that were stabilized by the CNF/NCh complexes resisted droplet creaming and coalescence of the oil phase. At intermediate NCh levels, the emulsions presented large droplet sizes while small droplets were observed at high NCh loadings, forming bimodal systems (NCh- and CNF/NCh-stabilized oil droplets). The adsorption of CNF/NCh complexes on the oil droplets can be tailored with NCh addition, owing to the increased affinity of acetyl groups in NCh with the oil phase, improving interfacial adsorption. Long-term stability (6-month storage) was

observed for CNF/NCh-stabilized emulsions. Under environmental stresses (e.g., pH 3-11 and 100-500 mM ionic strength), the size and morphology of emulsion droplets only showed slight changes, demonstrating the tolerance of the emulsions to the changes of pH and ionic strength. A mechanism explaining such superior stability of emulsions against environmental stresses relates to the interfacial adsorption and distribution of CNF in the complexes, which counteracts the charge losses caused by the deprotonation of NCh or charge screening of the complexes upon changing environmental conditions. Our results point to the possibility of *in situ* CNF modification strategy by complexation with cationic NCh, enabling a versatile design of stable all-renewable Pickering systems suitable for foodstuff and green products.

ASSOCIATED CONTENT

Supporting Information. Additional materials are provided related to TEM images of NCh and CNF; rheology of CNF/NCh-based Pickering emulsions; confocal images of emulsion after 1-day storage; dual-channel fluorescent images of emulsions; SEM images of polymerized polystyrene beads; visual appearance, droplet size, rheology, and confocal images of emulsions at varied oil fractions; optical images of emulsions at pH 9 and 11; confocal images of emulsions at different ionic strength; and visual appearance and confocal images of emulsions at varied oil fractions after 6-month storage.

AUTHOR INFORMATION

Corresponding Authors

* E-mail: orlando.rojas@ubc.ca Tel: +1-604-822-3457

* E-mail: siqi.huan@ubc.ca Tel: +1-236-869-0416

* E-mail: long.bai@ubc.ca Tel: +1-604-781-0416

Author Contributions

The manuscript was written through contributions of all authors. All authors have given approval to the final version of the manuscript.

ACKNOWLEDGMENTS

This work was supported by the Canada Excellence Research Chair initiative, European Research Council under the European Union's Horizon 2020 research and innovation program (ERC Advanced Grant No. 788489, "BioEICell"), and the Canada Foundation for Innovation (CFI). This work was also part of the Academy of Finland's Flagship Programme (Competence Center for Materials Bioeconomy, FinnCERES) under Projects No. 318890 and 318891.

REFERENCES

- (1) Bai, L.; Huan, S.; Gu, J.; McClements, D. J. Fabrication of Oil-in-Water Nanoemulsions by Dual-Channel Microfluidization Using Natural Emulsifiers: Saponins, Phospholipids, Proteins, and Polysaccharides. *Food Hydrocolloids* **2016**, *61*, 703-711.
- (2) Bai, L.; McClements, D. J. Formation and Stabilization of Nanoemulsions Using Biosurfactants: Rhamnolipids. *J. Colloid Interface Sci.* **2016**, *479*, 71-79.
- (3) McClements, D. J. *Food Emulsions: Principles, Practices, and Techniques*. CRC press: 2015.
- (4) Bai, L.; Huan, S.; Li, Z.; McClements, D. J. Comparison of Emulsifying Properties of Food-Grade Polysaccharides in Oil-in-Water Emulsions: Gum Arabic, Beet Pectin, and Corn Fiber Gum. *Food Hydrocolloids* **2017**, *66*, 144-153.
- (5) Ramsden, W. Separation of Solids in the Surface-Layers of Solutions and

- ‘Suspensions’(Observations on Surface-Membranes, Bubbles, Emulsions, and Mechanical Coagulation).-Preliminary account. *Proc. R. Soc. London* **1904**, 72, 156-164.
- (6) Pickering, S. U. Cxcvi.-Emulsions. *J. Chem. Soc., Trans.* **1907**, 91, 2001-2021.
- (7) Binks, B. P. Particles as Surfactants-Similarities and Differences. *Curr. Opin. Colloid Interface Sci.* **2002**, 7, 21-41.
- (8) Wu, J.; Ma, G. H. Recent Studies of Pickering Emulsions: Particles Make the Difference. *Small* **2016**, 12, 4633-4648.
- (9) Kalashnikova, I.; Bizot, H.; Cathala, B.; Capron, I. New Pickering Emulsions Stabilized by Bacterial Cellulose Nanocrystals. *Langmuir* **2011**, 27, 7471-7479.
- (10) Frelichowska, J.; Bolzinger, M.-A.; Chevalier, Y. Effects of Solid Particle Content on Properties of O/W Pickering Emulsions. *J. Colloid Interface Sci.* **2010**, 351, 348-356.
- (11) Arditty, S.; Whitby, C.; Binks, B.; Schmitt, V.; Leal-Calderon, F. Some General Features of Limited Coalescence in Solid-Stabilized Emulsions. *Eur. Phys. J. E* **2003**, 11, 273-281.
- (12) Lee, M. N.; Chan, H. K.; Mohraz, A. Characteristics of Pickering Emulsion Gels Formed by Droplet Bridging. *Langmuir* **2012**, 28, 3085-3091.
- (13) Jiao, B.; Shi, A.; Wang, Q.; Binks, B. P. High-Internal-Phase Pickering Emulsions Stabilized Solely by Peanut-Protein-Isolate Microgel Particles with Multiple Potential Applications. *Angewandte Chemie* **2018**, 130, 9418-9422.
- (14) Berton-Carabin, C. C.; Schroën, K. Pickering Emulsions for Food Applications: Background, Trends, and Challenges. *Annu. Rev. Food Sci. Technol.* **2015**, 6, 263-297.
- (15) Cai, X.; Wang, Y.; Du, X.; Xing, X.; Zhu, G. Stability of pH-Responsive Pickering Emulsion Stabilized by Carboxymethyl Starch/Xanthan Gum Combinations. *Food Hydrocolloids* **2020**, 109, 106093.
- (16) Li, W.; Suzuki, T.; Minami, H. The Interface Adsorption Behavior in A Pickering Emulsion Stabilized by Cylindrical Polystyrene Particles. *J. Colloid Interface Sci.* **2019**, 552, 230-235.
- (17) Dechézelles, J.-F. o.; Ciotonea, C.; Catrinescu, C.; Ungureanu, A.; Royer, S. b.; Nardello-Rataj, V. r. Emulsions Stabilized with Alumina-Functionalized Mesoporous Silica Particles.

- Langmuir* **2020**, *36*, 3212-3220.
- (18) McClements, D. J.; Bai, L.; Chung, C. Recent Advances in the Utilization of Natural Emulsifiers to Form and Stabilize Emulsions. *Annu. Rev. Food Sci. Technol.* **2017**, *8*, 205-236.
- (19) Bai, L.; Greca, L. G.; Xiang, W.; Lehtonen, J.; Huan, S.; Nugroho, R. W. N.; Tardy, B. L.; Rojas, O. J. Adsorption and Assembly of Cellulosic and Lignin Colloids at Oil/Water Interfaces. *Langmuir* **2019**, *35*, 571-588.
- (20) Bai, L.; Huan, S.; Zhao, B.; Zhu, Y.; Esquena, J.; Chen, F.; Gao, G.; Zussman, E.; Chu, G.; Rojas, O. J. All-Aqueous Liquid Crystal Nanocellulose Emulsions with Permeable Interfacial Assembly. *ACS Nano* **2020**, *14*, 13380-13390.
- (21) Bai, L.; Huan, S.; Zhu, Y.; Chu, G.; McClements, D. J.; Rojas, O. J. Recent Advances in Food Emulsions and Engineering Foodstuffs Using Plant-Based Nanocelluloses. *Annu. Rev. Food Sci. Technol.* **2021**, DOI: 10.1146/annurev-food-061920-123242.
- (22) Habibi, Y.; Lucia, L. A.; Rojas, O. J. Cellulose Nanocrystals: Chemistry, Self-Assembly, and Applications. *Chem. Rev.* **2010**, *110*, 3479-3500.
- (23) Bai, L.; Lv, S.; Xiang, W.; Huan, S.; McClements, D. J.; Rojas, O. J. Oil-in-Water Pickering Emulsions via Microfluidization with Cellulose Nanocrystals: 1. Formation and Stability. *Food Hydrocolloids* **2019**, *96*, 699-708.
- (24) Kalashnikova, I.; Bizot, H.; Bertoncini, P.; Cathala, B.; Capron, I. Cellulosic Nanorods of Various Aspect Ratios for Oil in Water Pickering Emulsions. *Soft Matter* **2013**, *9*, 952-959.
- (25) Goi, Y.; Fujisawa, S.; Saito, T.; Yamane, K.; Kuroda, K.; Isogai, A. Dual Functions of TEMPO-Oxidized Cellulose Nanofibers in Oil-in-Water Emulsions: A Pickering Emulsifier and A Unique Dispersion Stabilizer. *Langmuir* **2019**, *35*, 10920-10926.
- (26) Silva, C. E.; Tam, K. C.; Bernardes, J. S.; Loh, W. Double Stabilization Mechanism of O/W Pickering Emulsions Using Cationic Nanofibrillated Cellulose. *J. Colloid Interface Sci.* **2020**, *574*, 207-216.
- (27) Chakrabarty, A.; Teramoto, Y. Scalable Pickering Stabilization to Design Cellulose Nanofiber-Wrapped Block Copolymer Microspheres for Thermal Energy Storage. *ACS*

Sustainable Chem. Eng. **2020**, *8*, 4623-4632.

- (28) Gestranus, M.; Stenius, P.; Kontturi, E.; Sjöblom, J.; Tammelin, T. Phase Behaviour and Droplet Size of Oil-in-Water Pickering Emulsions Stabilised with Plant-Derived Nanocellulosic Materials. *Colloids Surf., A* **2017**, *519*, 60-70.
- (29) Li, Q.; Xie, B.; Wang, Y.; Wang, Y.; Peng, L.; Li, Y.; Li, B.; Liu, S. Cellulose Nanofibrils from Miscanthus Floridulus Straw As Green Particle Emulsifier for O/W Pickering Emulsion. *Food Hydrocolloids* **2019**, *97*, 105214.
- (30) Zhou, H.; Lv, S.; Liu, J.; Tan, Y.; Muriel Mundo, J. L.; Bai, L.; Rojas, O. J.; McClements, D. J. Modulation of Physicochemical Characteristics of Pickering Emulsions: Utilization of Nanocellulose-and Nanochitin-Coated Lipid Droplet Blends. *J. Agric. Food Chem.* **2019**, *68*, 603-611.
- (31) Bertsch, P.; Arcari, M.; Geue, T.; Mezzenga, R.; Nyström, G.; Fischer, P. Designing Cellulose Nanofibrils for Stabilization of Fluid Interfaces. *Biomacromolecules* **2019**, *20*, 4574-4580.
- (32) Huan, S.; Yokota, S.; Bai, L.; Ago, M.; Borghei, M.; Kondo, T.; Rojas, O. J. Formulation and Composition Effects in Phase Transitions of Emulsions Costabilized by Cellulose Nanofibrils and An Ionic Surfactant. *Biomacromolecules* **2017**, *18*, 4393-4404.
- (33) Lu, Y.; Qian, X.; Xie, W.; Zhang, W.; Huang, J.; Wu, D. Rheology of the Sesame Oil-in-Water Emulsions Stabilized by Cellulose Nanofibers. *Food Hydrocolloids* **2019**, *94*, 114-127.
- (34) Zhang, Y.; Wu, J.; Wang, B.; Sui, X.; Zhong, Y.; Zhang, L.; Mao, Z.; Xu, H. Cellulose Nanofibril-Reinforced Biodegradable Polymer Composites Obtained via A Pickering Emulsion Approach. *Cellulose* **2017**, *24*, 3313-3322.
- (35) Winuprasith, T.; Khomein, P.; Mitbumrung, W.; Suphantharika, M.; Nitithamyong, A.; McClements, D. J. Encapsulation of Vitamin D3 in Pickering Emulsions Stabilized by Nanofibrillated Mangosteen Cellulose: Impact on in Vitro Digestion and Bioaccessibility. *Food Hydrocolloids* **2018**, *83*, 153-164.
- (36) Aaen, R.; Simon, S.; Brodin, F. W.; Syverud, K. The Potential of TEMPO-Oxidized

- Cellulose Nanofibrils as Rheology Modifiers in Food Systems. *Cellulose* **2019**, *26*, 5483-5496.
- (37) Bai, L.; Huan, S.; Xiang, W.; Rojas, O. J. Pickering Emulsions by Combining Cellulose Nanofibrils and Nanocrystals: Phase Behavior and Depletion Stabilization. *Green Chem.* **2018**, *20*, 1571-1582.
- (38) Xu, H.-N.; Li, Y.-H.; Zhang, L. Driving Forces for Accumulation of Cellulose Nanofibrils at the Oil/Water Interface. *Langmuir* **2018**, *34*, 10757-10763.
- (39) Irvin, C. W.; Satam, C. C.; Liao, J.; Russo, P. S.; Breedveld, V.; Meredith, J. C.; Shofner, M. L. Synergistic Reinforcement of Composite Hydrogels with Nanofiber Mixtures of Cellulose Nanocrystals and Chitin Nanofibers. *Biomacromolecules* **2021**, *22*, 340-352.
- (40) Bai, L.; Xiang, W.; Huan, S.; Rojas, O. J. Formulation and Stabilization of Concentrated Edible Oil-in-Water Emulsions Based on Electrostatic Complexes of A Food-Grade Cationic Surfactant (Ethyl Lauroyl Arginate) and Cellulose Nanocrystals. *Biomacromolecules* **2018**, *19*, 1674-1685.
- (41) Ling, S.; Chen, W.; Fan, Y.; Zheng, K.; Jin, K.; Yu, H.; Buehler, M. J.; Kaplan, D. L. Biopolymer Nanofibrils: Structure, Modeling, Preparation, and Applications. *Prog. Polym. Sci.* **2018**, *85*, 1-56.
- (42) Bai, L.; Kämäräinen, T.; Xiang, W.; Majoinen, J.; Seitsonen, J.; Grande, R.; Huan, S.; Liu, L.; Fan, Y.; Rojas, O. J. Chirality from Cryo-Electron Tomograms of Nanocrystals Obtained by Lateral Disassembly and Surface Etching of Never-Dried Chitin. *ACS Nano* **2020**, *14* 6921-6930.
- (43) Duan, B.; Huang, Y.; Lu, A.; Zhang, L. Recent Advances in Chitin based Materials Constructed via Physical Methods. *Prog. Polym. Sci.* **2018**, *82*, 1-33.
- (44) Perrin, E.; Bizot, H.; Cathala, B.; Capron, I. Chitin Nanocrystals for Pickering High Internal Phase Emulsions. *Biomacromolecules* **2014**, *15*, 3766-3771.
- (45) Bai, L.; Huan, S.; Xiang, W.; Liu, L.; Yang, Y.; Nugroho, R. W. N.; Fan, Y.; Rojas, O. J. Self-Assembled Networks of Short and Long Chitin Nanoparticles for Oil/Water Interfacial Superstabilization. *ACS Sustainable Chem. Eng.* **2019**, *7*, 6497-6511.

- (46) Larbi, F.; García, A.; del Valle, L. J.; Hamou, A.; Puiggali, J.; Belgacem, N.; Bras, J. Comparison of Nanocrystals and Nanofibers Produced from Shrimp Shell α -Chitin: From Energy Production to Material Cytotoxicity and Pickering Emulsion Properties. *Carbohydr. Polym.* **2018**, *196*, 385-397.
- (47) Zhou, H.; Tan, Y.; Lv, S.; Liu, J.; Mundo, J. L. M.; Bai, L.; Rojas, O. J.; McClements, D. J. Nanochitin-Stabilized Pickering Emulsions: Influence of Nanochitin on Lipid Digestibility and Vitamin Bioaccessibility. *Food Hydrocolloids* **2020**, *106*, 105878.
- (48) Pang, K.; Ding, B.; Liu, X.; Wu, H.; Duan, Y.; Zhang, J. High-Yield Preparation of A Zwitterionically Charged Chitin Nanofiber and Its Application in A Doubly pH-Responsive Pickering Emulsion. *Green Chem.* **2017**, *19*, 3665-3670.
- (49) Huang, Y.; Liu, H.; Liu, S.; Li, S. Cinnamon Cassia Oil Emulsions Stabilized by Chitin Nanofibrils: Physicochemical Properties and Antibacterial Activities. *J. Agric. Food Chem.* **2020**, *68*, 14620-14631.
- (50) Kaku, Y.; Fujisawa, S.; Saito, T.; Isogai, A. Synthesis of Chitin Nanofiber-Coated Polymer Microparticles via Pickering Emulsion. *Biomacromolecules* **2020**, *21*, 1886-1891.
- (51) Huan, S.; Mattos, B. D.; Ajdary, R.; Xiang, W.; Bai, L.; Rojas, O. J. Two-Phase Emulgels for Direct Ink Writing of Skin-Bearing Architectures. *Adv. Funct. Mater.* **2019**, *29*, 1902990.
- (52) Lv, S.; Zhou, H.; Bai, L.; Rojas, O. J.; McClements, D. J. Development of Food-Grade Pickering Emulsions Stabilized by A Mixture of Cellulose Nanofibrils and Nanochitin. *Food Hydrocolloids* **2021**, *113*, 106451.
- (53) Facchine, E. G.; Bai, L.; Rojas, O. J.; Khan, S. A. Associative Structures Formed from Cellulose Nanofibrils and Nanochitins Are pH-Responsive and Exhibit Tunable Rheology. *J. Colloid Interface Sci.* **2021**, *588*, 232-241.
- (54) Zhu, Y.; Huan, S.; Bai, L.; Ketola, A.; Shi, X.; Zhang, X.; Ketoja, J. A.; Rojas, O. J. High Internal Phase Oil-in-Water Pickering Emulsions Stabilized by Chitin Nanofibrils: 3D Structuring and Solid Foam. *ACS Appl. Mater. Interfaces* **2020**, *12*, 11240-11251.
- (55) Huan, S.; Ajdary, R.; Bai, L.; Klar, V.; Rojas, O. J. Low Solids Emulsion Gels Based on

- Nanocellulose for 3D-Printing. *Biomacromolecules* **2018**, *20*, 635-644.
- (56) Liu, L.; Bai, L.; Tripathi, A.; Yu, J.; Wang, Z.; Borghei, M.; Fan, Y.; Rojas, O. J. High Axial Ratio Nanochitins for Ultrastrong and Shape-Recoverable Hydrogels and Cryogels via Ice Templating. *ACS Nano* **2019**, *13*, 2927-2935.
- (57) McClements, D. J. Critical Review of Techniques and Methodologies for Characterization of Emulsion Stability. *Crit. Rev. Food Sci. Nutr.* **2007**, *47*, 611-649.
- (58) Schneider, C. A.; Rasband, W. S.; Eliceiri, K. W. NIH Image to ImageJ: 25 Years of Image Analysis. *Nat. Methods* **2012**, *9*, 671-675.
- (59) Zhang, X.; Liu, Y.; Wang, Y.; Luo, X.; Li, Y.; Li, B.; Wang, J.; Liu, S. Surface Modification of Cellulose Nanofibrils with Protein Nanoparticles for Enhancing the Stabilization of O/W Pickering Emulsions. *Food Hydrocolloids* **2019**, *97*, 105180.
- (60) Werner, A.; Schmitt, V.; Sèbe, G.; Héroguez, V. Synthesis of Surfactant-Free Micro-and Nanolatexes from Pickering Emulsions Stabilized by Acetylated Cellulose Nanocrystals. *Polym. Chem.* **2017**, *8*, 6064-6072.

TABLE OF CONTENTS

Pickering Emulsions *via* Interfacial Nanoparticle Complexation of Oppositely Charged Nanopolysaccharides

Siqi Huan, Ya Zhu, Wenyang Xu, David Julian McClements, Long Bai, Orlando J. Rojas

NCh promotes interfacial adsorption of CNF/NCh complexes

